Finite Element Analysis for the Damage Detection of Light Pole Structures

Qixiang Tang[a], Tzuyang Yu[a] and Mark Jen[b]

[a]Department of Civil and Environmental Engineering
University of Massachusetts Lowell
One University Avenue, Lowell, MA 01854, U.S.A.
[b]Parsons Corporation
100 Broadway 18th FL, New York, NY 10005, U.S.A.

ABSTRACT

Failures of aging light poles can jeopardize the safety of residents and damage adjacent structures. The need for reliable and efficient damage detection methods is raised. Any change in structural properties (e.g., mass, stiffness and damping) can lead to differences in the dynamic response of structures (i.e., modal frequencies). As a result, changes in dynamic responses can be used as indicators for damage detection. In this study, relationships between artificial damages and modal frequencies are determined by investigating the modal frequencies of intact and damaged light pole models using the finite element method (FEM). Finite element (FE) models were built with 5,529 C3D8R elements in ABAQUS®. New parameters (sensitive and insensitive modes) were defined and used to evaluate the sensitivity of the first ten modes of FE models. It is found that combinations of sensitive and insensitive modes are unique for each damage location and can be used to locate artificial damages in light pole models. Empirical equations are proposed to quantify damage level and damage size.

Keywords: Finite element method (FEM), damage detection, light pole, sensitive modes, insensitive modes

1. INTRODUCTION

Aging of engineering structures, including light poles is inevitable and unstoppable. Light pole structures are installed in every modern city, and their failures can threaten public safety. In December 2009, a 200-pound corroded light pole fell across the southeast expressway in Massachusetts. Three other damaged poles were found and removed in the neighborhood right after the incident. The incident led to a daunting task to closely examining more than 4,000 poles in Massachusetts.[1] It is realized that current inspection techniques (e.g., acoustic, ultrasonic) are capable of detecting localized damages but inefficient to preform overall assessment. The need for reliable and efficient damage detection methods for light poles is evidential.

Damage detection using changes in the dynamic response of a structure (e.g. modal frequency and mode shape) is a popular approach in the nondestructive evaluation (NDE) and structural health monitoring (SHM) of engineering structures including light poles. Experimental and numerical studies have been reported in the literature. Three common damage (crack) locations in light poles were reported from a survey conducted by Roy et al.,[2] including 1) pole-to-transverse plate connection, 2) handhole detail and 3) anchor bolts. Le et al. [3] studied the relationships between modal frequencies of long tapered hollow poles and their geometric variables (e.g., pole length, top and bottom diameters of pole, bolt diameter) based on three-dimensional finite element analysis. By studying the couplings among material property, boundary condition and geometric nonlinearity, changes in pole geometry (length, thickness, diameter) were modeled using the first three modal frequencies of the pole. Owolabi et. al.[4] proposed an approach to relate the location and depth of a crack in fixed ended and simply supported beams, based on changes in modal frequencies and amplitudes of frequency response functions (FRF) of the beams. They found that modal frequency shift due to the presence of a crack depends not only on crack depth and crack location but also on vibration modes. Lee and Chung[5] reported a damage detection

---

Table 1. Material properties

	Pole and Baseplate	Bolts
Density	7.85×10^{-9} ton/mm^3	7.85×10^{-9} ton/mm^3
Young's Modulus	207×10^3 MPa	207×10^3 MPa
Poisson's ratio	0.3	0.3
Yield strength	450 MPa	250 MPa

procedure for locating cracks and identifying crack size in a one-dimensional Euler-Bernoulli cantilever beam the using first four modal frequencies. They determined the maximum stress in a damaged/cracked beam and estimated the approximate crack size by the ranking of mode numbers (Armon's rank-ordering method[6]). Actual crack location can be identified by Gudmundson's equation[7] using the determined maximum stress, crack size, and the first four modal frequencies.

In addition, recent advances in remote sensing technology have changed the inspection and monitoring practice in civil engineering. Techniques like scanning laser Doppler vibrometer (SLDV)[8] and digital image correlation (DIC)[9] enable inspection engineers to measure the vibration of structures in the field at ease. As a result, measuring modal frequencies and mode shapes of a structure will not be as tedious as it was before.

A damage detection method utilizing the coupling of vibration modes for detecting, locating, and quantifying three common damages in light pole structures is reported in this paper. Finite element method (FEM) is applied in building numerical light pole models and simulating free vibration of light pole models. A commercial finite element (FE) software package ABAQUS® (by Dassault Systems) is chosen for its wide applications in simulating the vibration of steel structures. Three artificial damages (crack locations) in a light pole are considered; i) pole-to-transverse plate connection, ii) top cross section of handhole and iii) bottom cross section of handhole. Modal frequencies and mode shapes are obtained from the free vibrations (eigenfrequency analysis) of intact and artificially damaged light pole models. In this development, two new modal parameters are defined; sensitive modes and insensitive modes. Combinations between sensitive and insensitive modes and modal frequency difference are used to i) detect damage, ii) locate damage, and iii) quantify damage.

In this paper, finite element modeling of intact and damaged light pole models is first described. Design of FE light pole models and the characterization of artificial damage are provided. In this research, three damage characteristic parameters for locating (L_j), sizing (α), and quantifying (β) damages in light pole structures are used. A step-by-step damage detection procedure based on the use of sensitive and insensitive modes and modal frequency difference is proposed. Finally, research findings are discussed and concluded.

2. FINITE ELEMENT MODELING

To verify the proposed damage detection method, numerical examples generated by finite element simulations are used. All FE light pole models are created by ABAQUS®. Dynamic responses of intact and artificially damaged light pole models are analyzed to extract their eigenfrequencies for identifying sensitive and insensitive modes for damage detection. Damaged light pole models are only different from intact light pole models by the addition of an artificial damage in each case, while sharing same geometry, material property, and boundary conditions with the intact model. The feasibility of modeling actual damages by changing the elastic modulus (Young's modulus) of model elements in numerical simulation has been reported.[10] Actual damages can be simulated by reducing the elastic modulus of model elements at the location where the damage is artificially introduced. FE modeling details are described in the following.

2.1 Intact Light Pole Models

All FE light pole models considered in this research are created based on a commercial product[11] (steel light pole) as shown in Fig. 1. Material properties of all FE light pole models are provided in Table 1. In the FE modeling of light pole structures, all FE light pole models are assembled by three main components: a round pole, a baseplate (Fig. 2), and four anchor bolts (Fig. 3). The round pole is hollow and tapered to the baseplate, with a height of six meters (19.68 ft). The size of the baseplate is $0.3 \times 0.3 \times 0.03$ m^3 ($0.98 \times 0.98 \times 0.098$ ft^3).

R0.028

0.25

0.105

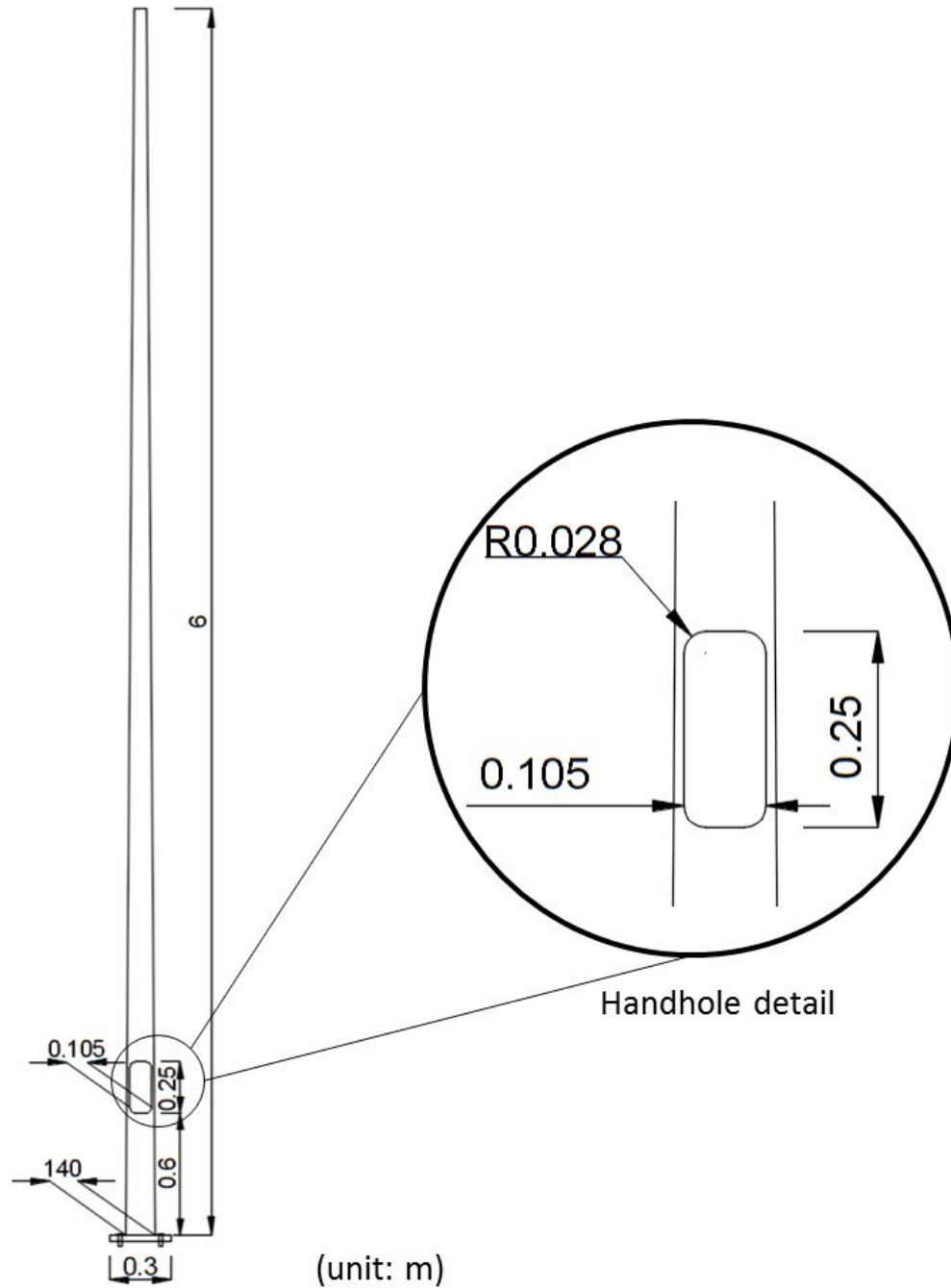Handhole detail

0.105

0.25

140

0.6

0.3

(unit: m)

Figure 1. Elevation view of the example light pole

The baseplate is bolted to the foundation with four anchor bolts Fig. 3. At the lower part of the round pole, a handhole opening is created on the pole, with an opening area of 0.25×0.105 m^2 (0.82×0.34 ft^2).

For dynamic analysis (i.e., eigenvalue-extraction), a solid linear elastic element (C3D8R) in ABAQUS® was selected. 5,529 elements were used in modeling a light pole structure, after performing a convergence study. The boundary conditions connecting the pole, the baseplate and the anchor bolts are shown in Fig. 4. The contact condition between the pole and the baseplate are simulated using tie constraint, as well as the contact condition

between the bolts and the baseplate. The anchor bolts are fixed to the foundation.
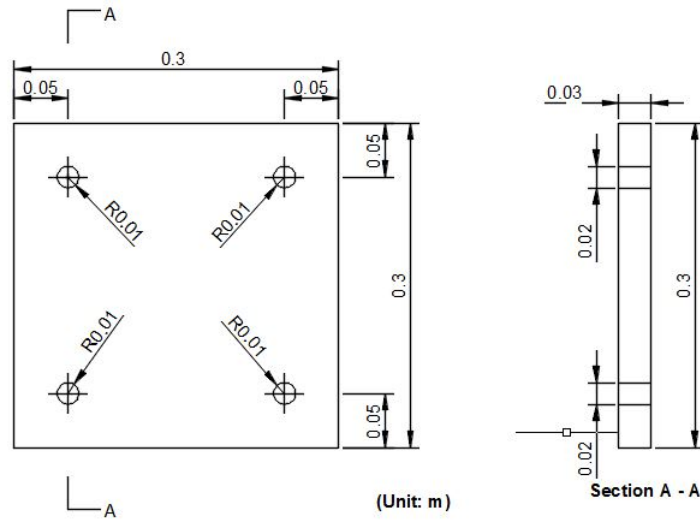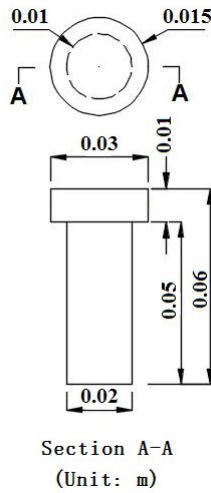

Figure 2. Plan view of the baseplate

Figure 3. Front view of the bolt

2.2 Damaged Light Pole Models

In the FE modeling of damaged light pole structures, three common damage locations are considered for artificial damages, including L_1, L_2 and L_3[2] (Fig. 5). Introduction of an artificial damage is achieved by reducing the Young's modulus of an element in the FE modeling of damaged light pole models (the smear method). Magnitude of an artificial damage is simulated by the number of elements. To characterize an artificial damage, three attributes are defined: damage location L_j, damage size αA and damage level βE. Both α and β are in the range of $[0, 1]$. These attributes are further explained in the following.

- Damage location, L_j ($j = 1, 2, 3$) - As shown in Fig. 5, L_1 is a horizontal damage at the top level of handhole, L_2 a horizontal damage at the bottom level of handhole, and L_3 a horizontal damage at the interface between the pole and the baseplate. No vertical damage is considered in this research.
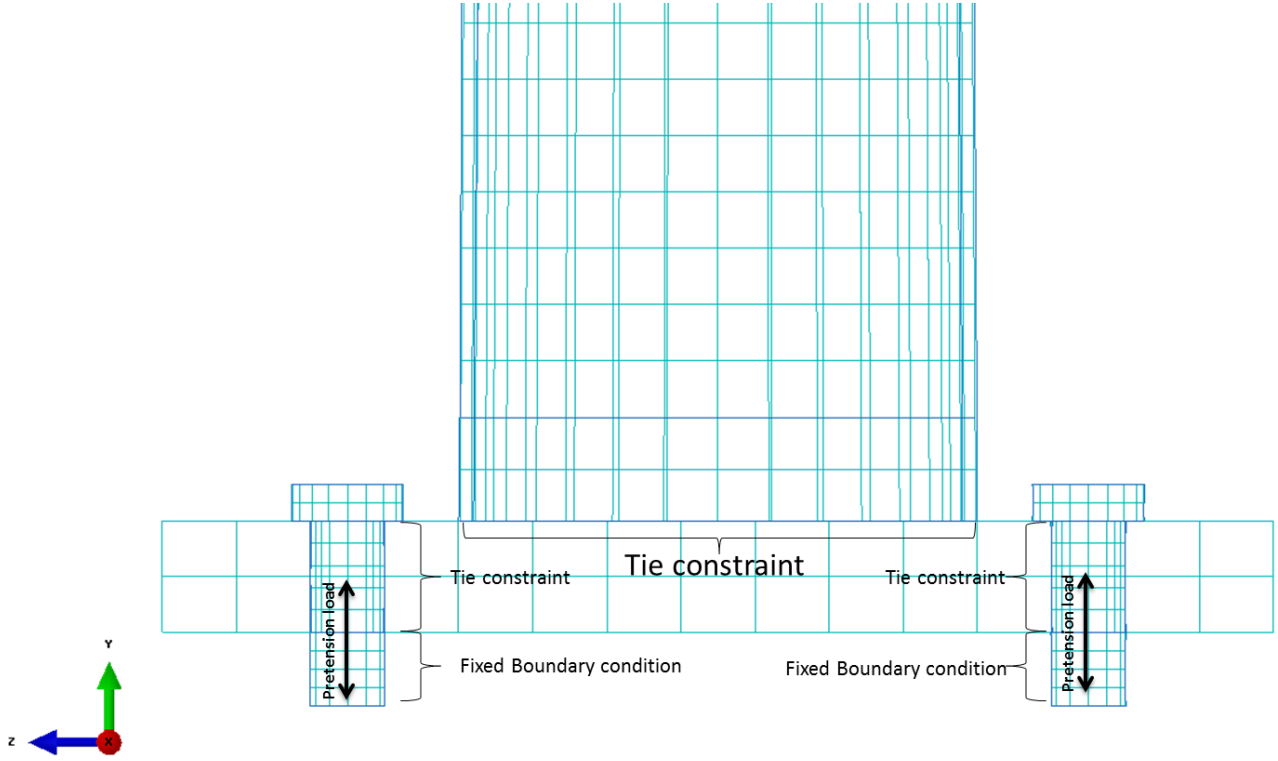
Figure 4. Boundary conditions in FE modeling

Table 2. Considered damage levels

β	Young's Modulus (GPa)
0.9	186.3
0.7	144.9
0.5	103.5
0.3	62.1
0.1	20.7

- Damage size, $\alpha \in [0, 1]$ - Damage size is quantified by α indicating the proportion of cross-sectional area A at a specified damage location L_j with reduced Young's modulus. Five damage sizes are considered in this research, $\alpha \in [0, 0.2, 0.4, 0.6, 0.8, 1]$ in which $\alpha = 0$ refers to an intact light pole model. Fig. 6 shows the cross-sectional view of different damage sizes at damage locations L_2 and L_3.

- Damage level, $\beta \in [0, 1]$ - Damage level is quantified by β to indicate the level of reduction in Young's modulus E for a specified damage size αA at a considered damage location L_j. Five damage levels are considered, $\beta = [0, 0.1, 0.3, 0.5, 0.7, 0.9]$, in which $\beta = 0$ refers to an intact light pole model. Table 2 lists the values of considered damage levels in this research.

For example, damage attributes combination $(L_j, \alpha A, \beta E) = (L_1, 0.2A, 0.7E)$ indicates a horizontal damage at the upper part of handhole with 20% of the total cross-sectional area consisted of 30%-reduced Young's modulus. Seventy-five combinations in total were created. Only one damage combination is considered at a time in each FE simulation case.

Eigenvalue analysis of intact and damaged FE light pole models provides the first fifty eigenfrequencies (modal frequencies) of each model. Considering practical difficulties associated with the measurement of higher modes, we used only the first ten modal frequencies in this research. Simulation results from the seventy-five cases are reported in the following section.
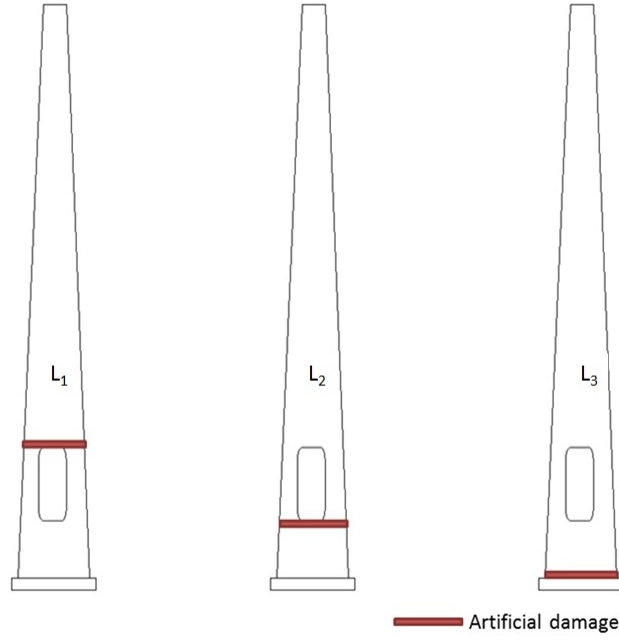
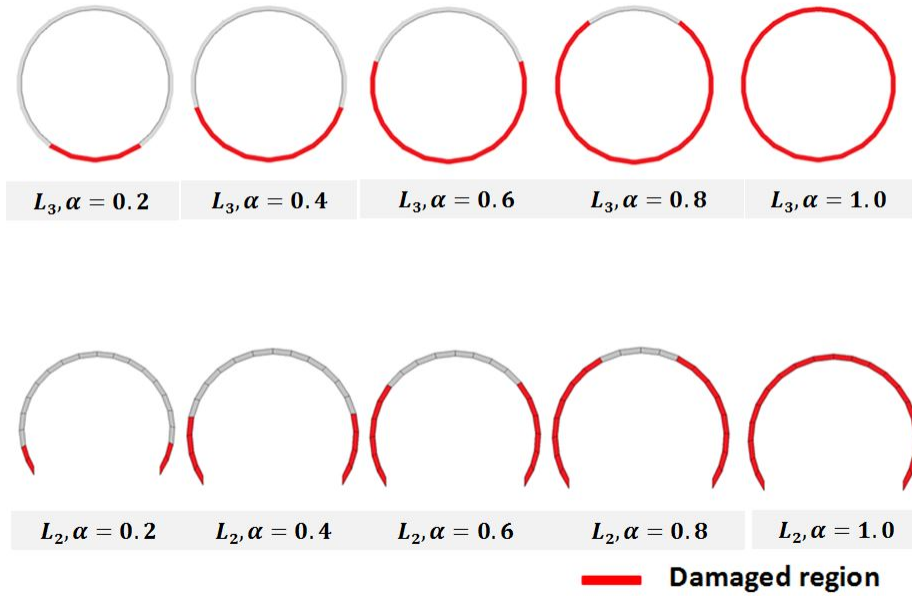Figure 5. Three considered damage/crack locations

Figure 6. Five stages of damages at L_3 and L_2

2.3 Modal Frequency Difference, Sensitive and Insensitive Modes

In this paper, modal frequency difference is defined by

$$\frac{\delta\omega_i^2}{\omega_i^2} = \frac{\omega_i^2 - (\omega_i^j)^2}{\omega_i^2} \qquad (1)$$

where ω_i^j is the ith mode eigenfrequency (modal frequency) of a damaged system, ω_i the ith mode eigenfrequency of an intact system. Sensitive modes n_s are determined by

$$n_s = \left[i, \frac{\delta\omega_i^2}{\omega_i^2} > \left(\frac{\delta\omega_i^2}{\omega_i^2} \right)_s \middle| i \in \mathbb{Z} \right] \tag{2}$$

in which $\left(\dfrac{\delta\omega_i^2}{\omega_i^2} \right)_s$ is the threshold value of $\left(\dfrac{\delta\omega_i^2}{\omega_i^2} \right)$ for sensitive modes. Similarly, insensitive modes n_{is} are determined by

$$n_{is} = \left[i, \frac{\delta\omega_i^2}{\omega_i^2} < \left(\frac{\delta\omega_i^2}{\omega_i^2} \right)_{is} \middle| i \in \mathbb{Z} \right] \tag{3}$$

in which $\left(\dfrac{\delta\omega_i^2}{\omega_i^2} \right)_{is}$ is the threshold value of $\left(\dfrac{\delta\omega_i^2}{\omega_i^2} \right)$ for insensitive modes. In the following sections, FE simulation is used to demonstrate the feasibility of the proposed damage detection method.

3. SIMULATION RESULTS

3.1 Modal Frequency Difference

Figs. 7, 8, and 9 show the modal frequency difference $\left(\dfrac{\delta\omega_i^2}{\omega_i^2} \right)$ in the first ten modes of three damage locations in which damage size $\alpha = 1$ (entire cross-sectional area) and damage level $\beta = 0.5$ (50% reduction in Young's modulus). Thresholds for modal frequency difference $\left(\dfrac{\delta\omega_i^2}{\omega_i^2} \right)_s$ in sensitive modes are selected as follows.

$$L_1 : \left(\frac{\delta\omega_i^2}{\omega_i^2} \right)_s = 1.25 \cdot \left(\frac{\delta\omega_i^2}{\omega_i^2} \right)_{avg} = 0.01478 \tag{4}$$

$$L_2 : \left(\frac{\delta\omega_i^2}{\omega_i^2} \right)_s = 1.25 \cdot \left(\frac{\delta\omega_i^2}{\omega_i^2} \right)_{avg} = 0.01452 \tag{5}$$

$$L_3 : \left(\frac{\delta\omega_i^2}{\omega_i^2} \right)_s = 1.25 \cdot \left(\frac{\delta\omega_i^2}{\omega_i^2} \right)_{avg} = 0.01057 \tag{6}$$

where $\left(\dfrac{\delta\omega_i^2}{\omega_i^2} \right)_{avg}$ is the arithmetic mean of $\dfrac{\delta\omega_i^2}{\omega_i^2}$ for the first ten modes. For the thresholds of insensitive modes,

$$L_1 : \left(\frac{\delta\omega_i^2}{\omega_i^2} \right)_{is} = 0.4 \cdot \left(\frac{\delta\omega_i^2}{\omega_i^2} \right)_{avg} = 0.0532 \tag{7}$$

$$L_2 : \left(\frac{\delta\omega_i^2}{\omega_i^2} \right)_{is} = 0.4 \cdot \left(\frac{\delta\omega_i^2}{\omega_i^2} \right)_{avg} = 0.00523 \tag{8}$$

$$L_3 : \left(\frac{\delta\omega_i^2}{\omega_i^2} \right)_{is} = 0.4 \cdot \left(\frac{\delta\omega_i^2}{\omega_i^2} \right)_{avg} = 0.00381 \tag{9}$$

3.2 Sensitive and Insensitive Modes

From the FE simulation, thresholds for sensitive and insensitive modes were selected such that the numbers of sensitive and insensitive modes are small enough for the ease in practical damage detection and health monitoring. Tables 3-8 list all the sensitive modes for three damage locations (L_1, L_2, L_3) with five damage sizes ($\alpha = [0.2, 0.4, 0.6, 0.8, 1.0]$). The mutual sensitive/insensitive modes of each damage location are summarized in Table 9, using the thresholds in Eqs.(4)-(9).

Table 3. Sensitive modes for damage location L_1

Damage location	α (with $\beta = 0.5$)	Sensitive modes	β (with $\alpha = 1.0$)	Sensitive modes
L_1	0.2	1,5,7	0.9	1,5,7
	0.4	1,5,7	0.7	1,5,7
	0.6	1,5,7	0.5	1,57
	0.8	1,5,7	0.3	1,7
	1.0	1,5,7	0.1	1,2,7
Mutual sensitive modes = 1,7				

Table 4. Insensitive modes for damage location L_1

Damage location	α (with $\beta = 0.5$)	Insensitive modes	β (with $\alpha = 1.0$)	Insensitive modes
L_1	0.2	3,6	0.9	3,6,8
	0.4	3,6,8	0.7	3,6,8
	0.6	3,6,8	0.5	3,6,8
	0.8	3,6	0.3	6,8
	1.0	3,6,8	0.1	6,8
Mutual insensitive modes = 6				

Table 5. Sensitive modes for damage location L_2

Damage location	α (with $\beta = 0.5$)	Sensitive modes	β (with $\alpha = 1.0$)	Sensitives modes
L_2	0.2	1,5,7	0.9	1,5,7
	0.4	1,5,7	0.7	1,5,7
	0.6	1,5,7	0.5	1,5,7
	0.8	1,5,7	0.3	1,5,7
	1.0	1,5,7	0.1	1,2,7
Mutual sensitive modes = 1,7				

Table 6. Insensitive modes for damage location L_2

Damage location	α (with $\beta = 0.5$)	Insensitive modes	β (with $\alpha = 1.0$)	Insensitive modes
L_2	0.2	2,4,8,10	0.9	6,8,10
	0.4	6,8,10	0.7	6,8,10
	0.6	6,8,10	0.5	6,8,10
	0.8	6,8,10	0.3	6,8,10
	1.0	6,8,10	0.1	6,8,10
Mutual insensitive modes = 8,10				

Table 7. Sensitive modes for damage location L_3

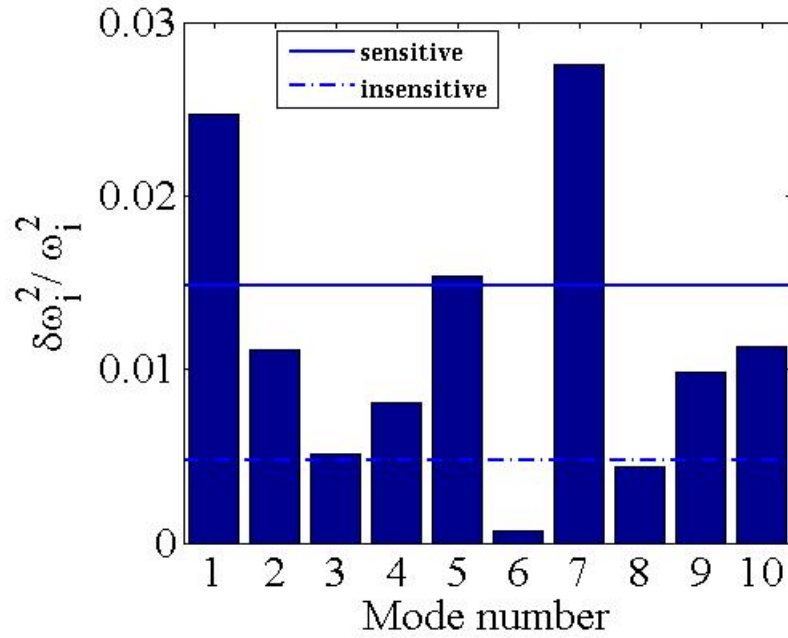| Damage location	α (with $\beta = 0.5$)	Sensitive modes	β (with $\alpha = 1.0$)	Sensitives modes
L_3	0.2	1,6,8,10	0.9	4,9,10
	0.4	8,9,10	0.7	4,9,10
	0.6	2,9,10	0.5	4,9,10
	0.8	2,4,9,10	0.3	4,9,10
	1.0	2,4,9,10	0.1	2,4,9,10
Mutual sensitive modes = 10				

Figure 7. Modal frequency differences at location L_1
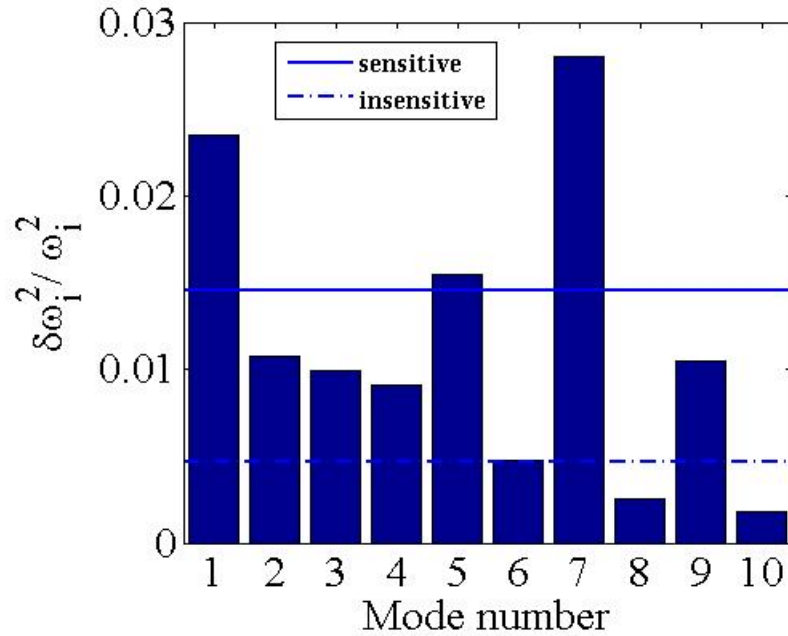
Figure 8. Modal frequency differences at location L_2

3.3 Damage Detection

In this paper, damage detection is achieved by the use of sensitive and insensitive modes and modal frequency difference, which is explained in the following paragraphs.

- Damage location, L_j – Combinations of mutual sensitive and insensitive modes are used to locate damage. For example, in Table 9, damage location L_1 is confirmed when i) modes 1 and 7 are identified to be
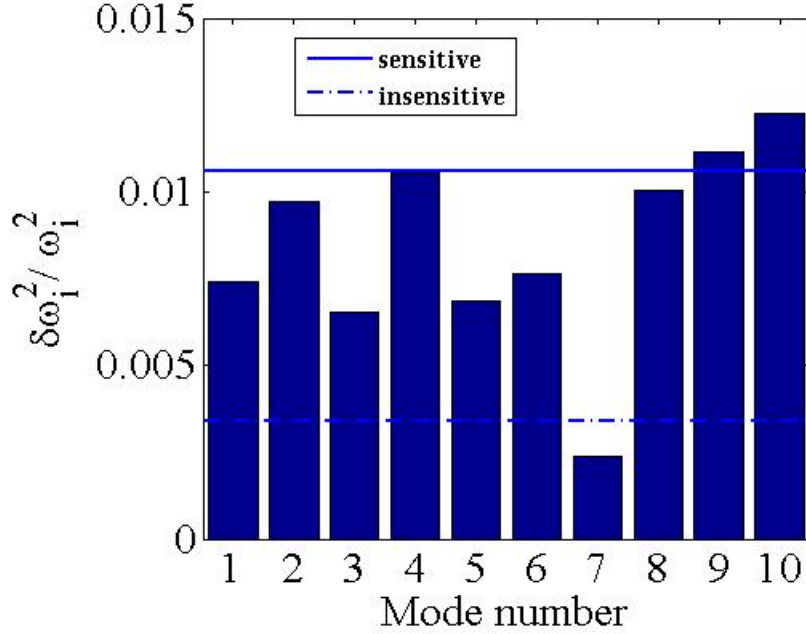
Figure 9. Modal frequency differences at location L_3

Table 8. Insensitive modes for damage location L_3

Damage location	α (with $\beta = 0.5$)	Insensitive modes	β (with $\alpha = 1.0$)	Insensitive modes
	0.2	2,4,5,7	0.9	7
	0.4	5,7	0.7	7
L_3	0.6	7	0.5	7
	0.8	7	0.3	7
	1.0	7	0.1	7
	Mutual insensitive modes = 7			

sensitive modes and ii) mode 6 is identified to be an insensitive mode. Criteria for locating all considered damage locations are provided as follows:

$$L_1 : [n_s = (1,7) \cap n_{is} = (6)] \tag{10}$$
$$L_2 : [n_s = (1,7) \cap n_{is} = (8,10)] \tag{11}$$
$$L_3 : [n_s = (9,10) \cap n_{is} = (7)] \tag{12}$$

- Damage size, αA – To determine the damaged area at a specified damage location, modal frequency difference is used. Tables 10, 11 and 12 list the modal frequency differences of first ten modes with five damage sizes ($\alpha = [0.2, 0.4, 0.6, 0.8, 1.0]$) at three damage locations L_1, L_2, and L_3, respectively. In these tables, damage level β is 0.5 (50%). Criteria for determining damage size at three damage locations are as

Table 9. Sensitive and insensitive modes for all damage locations

Location	Sensitive modes	Insensitive modes
L_1	1, 7	6
L_2	1, 7	8, 10
L_3	10	7

follows:

$$L_1 : \alpha = 463.059 \left(\frac{\delta \omega_4^2}{\omega_4^2} \right) - 2.819 \tag{13}$$

$$L_2 : \alpha = 414.526 \left(\frac{\delta \omega_9^2}{\omega_9^2} \right) - 3.3723 \tag{14}$$

$$L_3 : \alpha = 77.871 \left(\frac{\delta \omega_2^2}{\omega_2^2} \right) + 0.1783 \tag{15}$$

Note that the subscript indicates the mode number. The reason for choosing specific mode in Eqs. (13)-(15) is because of their high R-squared values (also provided in Tables 10, 11 and 12).

Table 10. Modal frequency differences for location L_1

Mode	α=0.2	α=0.4	α=0.6	α=0.8	α=1.0	R^2
1	0.015938	0.018643	0.019216	0.021226	0.024688	0.950832
2	0.004819	0.007728	0.009727	0.010863	0.011113	0.900609
3	0.002775	0.003595	0.003715	0.004222	0.005101	0.948772
4	0.006485	0.006962	0.007416	0.00794	0.008115	0.980942
5	0.011589	0.014342	0.015128	0.015303	0.015399	0.719262
6	0.000236	0.000513	0.000587	0.000638	0.000707	0.85732
7	0.016658	0.024422	0.027118	0.027459	0.027541	0.713196
8	0.003556	0.003914	0.004136	0.004253	0.004392	0.944514
9	0.007011	0.008761	0.00939	0.009641	0.009868	0.819153
10	0.009264	0.010045	0.010428	0.010811	0.011301	0.978673

Table 11. Modal frequency differences for location L_2

Mode	α=0.2	α=0.4	α=0.6	α=0.8	α=1.0	R^2
1	0.01544	0.017408	0.017952	0.019941	0.023492	0.932396
2	0.00277	0.006841	0.009431	0.010548	0.010768	0.86513
3	0.007183	0.007809	0.008073	0.008771	0.009948	0.944533
4	0.002347	0.006404	0.008452	0.008987	0.00908	0.795648
5	0.010475	0.013956	0.015208	0.015394	0.015474	0.728473
6	0.003796	0.004045	0.004243	0.004446	0.004709	0.99739
7	0.023796	0.026041	0.026999	0.02773	0.028007	0.884807
8	0.00187	0.002229	0.002446	0.002495	0.0025	0.805671
9	0.00853	0.009182	0.009643	0.010119	0.01044	0.985962
10	0.0006	0.001293	0.001524	0.001616	0.00177	0.841782

- Damage level, βE – To determine the damage level of a damaged area at a specified damage location, modal frequency difference is used. Tables 13, 14 and 15 list the modal frequency differences of the first ten modes with five damage levels at three damage locations, L_1, L_2, and L_3, respectively. In all these cases, full cross sectional area was considered damaged ($\alpha = 1$). Criteria for determining damage size at

Table 12. Modal frequency differences for location L_3

Mode	α=0.2	α=0.4	α=0.6	α=0.8	α=1.0	R^2
1	0.001629	0.002891	0.003133	0.003846	0.00742	0.823353
2	0.000387	0.002454	0.005682	0.008825	0.009727	0.975332
3	0.001545	0.002691	0.002884	0.003571	0.006534	0.839056
4	0.000304	0.002008	0.005332	0.009313	0.010557	0.974954
5	0.000121	0.00057	0.00235	0.005639	0.006862	0.944492
6	0.001862	0.003242	0.003486	0.004349	0.007634	0.857184
7	0.000377	0.001461	0.001816	0.002109	0.002365	0.889974
8	0.002458	0.004287	0.00464	0.00588	0.010047	0.871415
9	0.000858	0.004896	0.008785	0.010578	0.011159	0.919814
10	0.003416	0.005521	0.005935	0.007869	0.012251	0.900628

Table 13. Modal frequency differences for location L_1

Mode	β=0.9	β=0.7	β=0.5	β=0.3	β=0.1	R^2
1	0.002992	0.011117	0.024688	0.053185	0.164327	0.990478
2	0.001272	0.004849	0.011113	0.025097	0.086968	0.991168
3	0.000616	0.002293	0.005101	0.011017	0.034056	0.990533
4	0.001016	0.003723	0.008115	0.01681	0.047029	0.989155
5	0.002068	0.007385	0.015399	0.029644	0.068346	0.983596
6	9.24E-05	0.000337	0.000707	0.0014	0.003768	0.986589
7	0.003794	0.013407	0.027541	0.051757	0.114048	0.981388
8	0.000562	0.002041	0.004392	0.008941	0.024186	0.98838
9	0.001398	0.004885	0.009868	0.018049	0.037651	0.97829
10	0.001416	0.005213	0.011301	0.023239	0.063302	0.988446

three damage locations are as follows:

$$L_1 : \beta_2 = -0.196 \ln \left(\frac{\delta\omega_2^2}{\omega_2^2} \right) + 0.389 \tag{16}$$

$$L_2 : \beta_2 = -0.195 \ln \left(\frac{\delta\omega_2^2}{\omega_2^2} \right) - 0.388 \tag{17}$$

$$L_3 : \beta_8 = -0.199 \ln \left(\frac{\delta\omega_8^2}{\omega_8^2} \right) - 0.424 \tag{18}$$

Note that the subscript indicates the mode number. Specific modes are selected in Eqs. (16)-(18) due to their high R-squared values (Tables 13, 14 and 15).

4. SUMMARY AND DISCUSSION

From the FE simulation cases, it is found that the combination of sensitive and insensitive modes is unique for each damage location considered in this paper. Once the location of damage is determined or estimated, specific modal frequency change can be used to assess damage size (Eqs.(13)-(15)) and damage level (Eqs.(16)-(18)). The proposed damage detection method is summarized and discussed in the following.

- Procedure of the proposed damage detection method:

Table 14. Modal frequency differences for location L_2

Mode	β=0.9	β=0.7	β=0.5	β=0.3	β=0.1	R^2
1	0.002838	0.010559	0.023492	0.050845	0.159429	0.990579
2	0.001227	0.004689	0.010768	0.024456	0.086377	0.991129
3	0.001219	0.004523	0.009948	0.021018	0.061216	0.989736
4	0.001121	0.004143	0.00908	0.019207	0.057618	0.98986
5	0.002078	0.007415	0.015474	0.029962	0.070425	0.984399
6	0.000601	0.00219	0.004709	0.009609	0.025678	0.988229
7	0.00384	0.013582	0.028007	0.053084	0.118866	0.982338
8	0.000337	0.001196	0.0025	0.004874	0.011876	0.985728
9	0.001449	0.0051	0.01044	0.019578	0.043435	0.981667
10	0.000231	0.000831	0.00177	0.0036	0.010704	0.988751

Table 15. Modal frequency differences for location L_3

Mode	β=0.9	β=0.7	β=0.5	β=0.3	β=0.1	R^2
1	0.000844	0.003221	0.00742	0.01694	0.060623	0.991206
2	0.001107	0.004227	0.009727	0.022179	0.07883	0.99121
3	0.000736	0.002835	0.006534	0.014844	0.051704	0.99118
4	0.001215	0.004621	0.010557	0.023726	0.079334	0.991287
5	0.000802	0.003026	0.006862	0.015118	0.047321	0.9911
6	0.000873	0.00333	0.007634	0.017252	0.058737	0.99133
7	0.000281	0.001056	0.002365	0.005076	0.014748	0.990134
8	0.001155	0.004394	0.010047	0.022518	0.0739	0.991338
9	0.001285	0.004889	0.011159	0.024912	0.080553	0.991259
10	0.001416	0.005382	0.012251	0.027161	0.084875	0.991143

1. Collect the first ten modal frequencies of an intact light pole structure.

2. Measure the first ten modal frequencies of a damaged light pole structure.

3. Calculate the modal frequency difference $\left(\dfrac{\delta\omega_i^2}{\omega_i^2}\right)$ to detect the presence of damage.

4. Define the thresholds for sensitive $\left(\dfrac{\delta\omega_i^2}{\omega_i^2}\right)_s$ and insensitive $\left(\dfrac{\delta\omega_i^2}{\omega_i^2}\right)_{is}$ modes from numerical simulation (e.g., finite element analysis) in order to determine the sensitive (n_s) and insensitive (n_{is}) modes.

5. Use the combination of sensitive and insensitive modes to locate damage.

6. Use the modal frequency difference to quantify the size and the level of damage.

- Damage location - It is found that the combination of sensitive modes and insensitive modes is unique for each damage location. By checking the combination of sensitive and insensitive modes of an unknown damaged light pole, one can locate the damage in the light poles. In other words, the combination of sensitive and insensitive modes can be used as a damage indicator for locating damages.

- Damage size and damage level - Using predetermined relationships between modal frequency difference and damage characteristic parameters α and β, damage size and damage level can be estimated at considered damage locations.

5. CONCLUSION

In this paper, a step-by-step damage detection method utilizing the combination of sensitive and insensitive modes $(n_s$ and $n_{is})$ and modal frequency difference $\left(\dfrac{\delta\omega_i^2}{\omega_i^2}\right)$ is reported for detecting, locating, and quantifying damages in light pole structures. Feasibility of the proposed damage detection method is verified by FE simulation. The use of multiple sensitive and insensitive modes and their unique combination allows engineers to target at certain eigenfrequency modes, avoiding the difficulties associated with using single, varying eigenfrequency for damage detection. It is believed that this method has a great potential to be applied to the damage detection and structural health monitoring of light pole structures in practice.

6. ACKNOWNLEDGEMENT

REFERENCES

[1] Shortsleeve, J., "I-team: Aging light poles a safety concern on Mass. roads," CBS, $<$http://boston.cbslocal.com/2012/10/31/i-team-aging-light-poles-a-safety-concern-on-mass-roads$>$.

[2] Roy, S., Ocel, Y. C., Sause, R., Fisher, J. W., and J.Kaufmann, E., "Cost-effective connection details for highway sign, luminaire, and traffic signal structures," Tech. Rep. NCHRP 10-70, Advanced Technology for Large Structural Systems (ATLSS) Center (2011).

[3] Lea, T., Abolmaalia, A., Motaharia, S. A., Yeihb, W., and Fernandezc, R., "Finite element-based analyses of natural frequencies of long tapered hollow steel poles," Journal of Constructional Steel Research 64, 275–284 (2008).

[4] Owolabi, G. M., Swamidas, A. S. J., and Seshadri, R., "Crack detection in beams using changes in frequencies and amplitudes of frequency response functions," Journal of Sound and Vibration 265, 1–22 (2003).

[5] Lee, Y. and Chung, M., "A study on crack detection using eigenfrequency test data," Computers and Structures 64, 327–342 (2000).

[6] Armon, D., Ben-Haim, Y., and Braun, S., "Crack detection in beams by rank-ordering of eigenfrequency shift," Mechanical Systems and Signal Processing 8, 81–91 (1994).

[7] Gudmundson, P., "Eigenfrequency changes of strutures due to cracks, notches or other geometrical changes," Journal of Mechanics and Physics of Solids 30, 339–53 (1982).

[8] Yu, T.-Y., "Laser-based sensing," in [Sensor Technologies for Civil Infrastructures: Performance Assessment and Health Monitoring], Wang, M. L., Lynch, J. P., and Sohn, H., eds., ch. 12, Woodhead Publishing, Waltham, MA (2014).

[9] Nonis, C., Niezrecki, C., Yu, T.-Y., Ahmed, S., Su;, C., and Schmidt, T., "Structural health monitoring of bridges using digital image correlation," Proc. SPIE 8695 , 193–199 (2013).

[10] Yan, Y. J., Yam, L. H., Cheng, L., and Yu, L., "FEM modeling method of damage structures for structural damage detection," Composite Structures 72, 193–199 (2006).

[11] "Lighting poles and masts." Elektromonta Rzeszw SA, <`http://www.elektromontaz.com.pl/img/produkty_211_109_eng2.pdf`>.